ARTICLE IN PRESS

Progress in Solid State Chemistry xxx (xxxx) xxx



Contents lists available at ScienceDirect

Progress in Solid State Chemistry

journal homepage: www.elsevier.com/locate/pssc



Understanding color variation with site distribution in inverse spinel structure via neutron diffraction, magnetism, and optical studies

Anjali Verma^a, Jun Li^a, Arthur P. Ramirez^b, M.A. Subramanian^{a,*}

ARTICLE INFO

Keywords:
Chromophores
Intense pigments
Inverse spinel structure
Neutron refinement

ABSTRACT

Chromophores at different coordinations can give rise to different colors; usually, chromophores at noncentrosymmetric coordinations are preferred for intense pigments. Different solid solutions $M_{2-x}Co_xM'O_4$ (M = Mg/Zn, and M' = Ti/Sn) with inverse spinel structure were synthesized with the goal of understanding color variation with site distribution, as the chromophore Co²⁺ in these solid solutions can occupy either the tetrahedral or octahedral sites or both depending on the composition. Another goal was to develop environmentally friendly and cheap blue pigments by reducing the carcinogenic cobalt to obtain a similar color to that of commercially available cobalt blue, which uses a significant amount of Co²⁺ (33.31 % by mass). For Mg₂₋ _xCo_xTiO₄ series, turquoise blue hues were observed for low cobalt content, and different shades of blue were observed for Mg_{2.x}Co_xSnO₄ series with a color similar to cobalt blue, including just 4.90% of cobalt by mass. While for Zn2-xCoxTiO4, and Zn2-xCoxSnO4 series, different shades of brown and different shades of green, respectively, were observed. One of the main reasons behind the major difference in color for the Mg and Zn containing solid solutions, regardless of the same chromophore in the same structure is related to the chromophore site distribution in the system. For the Mg-containing solid solutions, different shades of blue are observed as Mg has no preference for any of the sites, Co²⁺ mostly goes to tetrahedral sites. In contrast, for the Zncontaining solid solutions, no blue shades were observed because of the strong preference of Zn for the tetrahedral sites owing to the sp³ hybridization, which in turn forces Co²⁺ to occupy the octahedral sites. Neutron refinement proves that Co^{2+} occupies mainly tetrahedral sites in the Mg-containing solid solutions and mostly octahedral sites in the Zn-containing solid solutions.

1. Introduction

Rationally creating an intense colorant has been a challenge for centuries [1]. The origin of color in gemstones and minerals has been extensively studied [2–4]. Still, it is difficult to predict the color in solids simply by any one of the known chemical and physical mechanisms which are responsible for observed colors [1].

Compared to dyes, inorganic pigments are promising because of their durability in different environments [5,6]. The current approaches to predict color in new inorganic materials transcend the conventional attribution of colors to certain elements in the solid (greenish blue colors to copper, deep blue to cobalt, red to lead or cadmium, or green to chromium or nickel), which can often be incorrect [7]. Instead, in Prussian blue, cobalt blue, and YInMn blue, the blue color comes from different chromophores in different coordinations. For intense pigments,

chromophores at non-centrosymmetric coordinations are preferred, such as tetrahedral, trigonal bipyramidal, etc. In some cases, the same chromophore in different structures (for example, ${\rm Cr}^{3+}$ in ruby and emerald [2]) or the same chromophore in the same structure at different coordinations can give rise to different colors.

Currently, there is an ongoing quest for a blue pigment that is nontoxic, durable, and cheap [8]. Making a blue pigment has always required either hard work or a stroke of luck [9]. The first blue material discovered was lapis lazuli about 6000 years ago [9]. The problem with lapis lazuli was its cost. In 1706, a German dye maker, John Jacob Diesbach, accidently made Prussian blue (Fe₄[Fe(CN)₆]₃) [9]. In 1802, pure cobalt blue pigment (CoAl₂O₄) was synthesized by a French chemist, although mixtures containing cobalt blue had previously been used in Chinese porcelain [10,11]. After 200 years, YInMn blue was accidently discovered while searching for magnetodielectric materials,

E-mail address: mas.subramanian@oregonstate.edu (M.A. Subramanian).

https://doi.org/10.1016/j.progsolidstchem.2024.100455

Received 10 February 2024; Received in revised form 28 March 2024; Accepted 31 March 2024 Available online 4 April 2024 0079-6786/© 2024 Elsevier Ltd. All rights reserved.

^a Department of Chemistry, Oregon State University, Corvallis, OR, 97331, USA

b Department of Physics, University of California, Santa Cruz, CA, 95064, USA

^{*} Corresponding author.

sparking a renewed worldwide interest in pigment discovery [9,12]. Most of these compounds suffer from toxicity, stability, color, or cost issues [9,13]. Out of all CoAl2O4, emerged as a dominant commercial blue pigment for the past 200 years; its color is attributed to the d-d transition of tetrahedral Co²⁺ [14]. CoAl₂O₄ crystallizes in the normal spinel structure. Spinels are one of the fascinating structures, with the general formula AM_2O_4 [15]. They generally crystallize in a cubic lattice with space group $Fd \overline{3} m$ (Fig. 1). It is known for showing many different properties and has been widely used as a host for pigments and interesting or unusual magnetic behavior [16,17]. It crystallizes in two forms, normal and inverse; in both forms, oxygen occupies the cubic close packing while cations occupy the tetrahedral, and octahedral sites; the only difference between them is the distribution of cations; for the normal spinel structure AM_2O_4 , A occupies the tetrahedral site while M occupies only the octahedral site, whereas, for the inverse spinel structure, AM_2O_4 ($M(AM)O_4$) A occupies the octahedral site while M occupies both sites [15], which makes the inverse spinel structure worthy of investigation for understanding the site distribution with color, and also for obtaining intense pigments with tunable hues, since any substituted ions at the M site can occupy either or both of the sites (Fig. 1).

We have investigated the solid solutions $M_{2-x}\mathrm{Co}_xM'\mathrm{O}_4$ ($M=\mathrm{Mg/Zn}$, $M'=\mathrm{Ti/Sn}$) with inverse spinel structure with the goal to do a systematic study on how the site distribution affects the color and with another goal to develop environmentally friendly and cheap blue pigments by reducing the carcinogenic cobalt to get a similar color to commercially available cobalt blue which uses a considerable amount of carcinogenic Co^{2+} . We have found that the Mg-containing solid solutions shows various shades of turquoise blue (Mg_{2-x}Co_xTiO₄), and blue

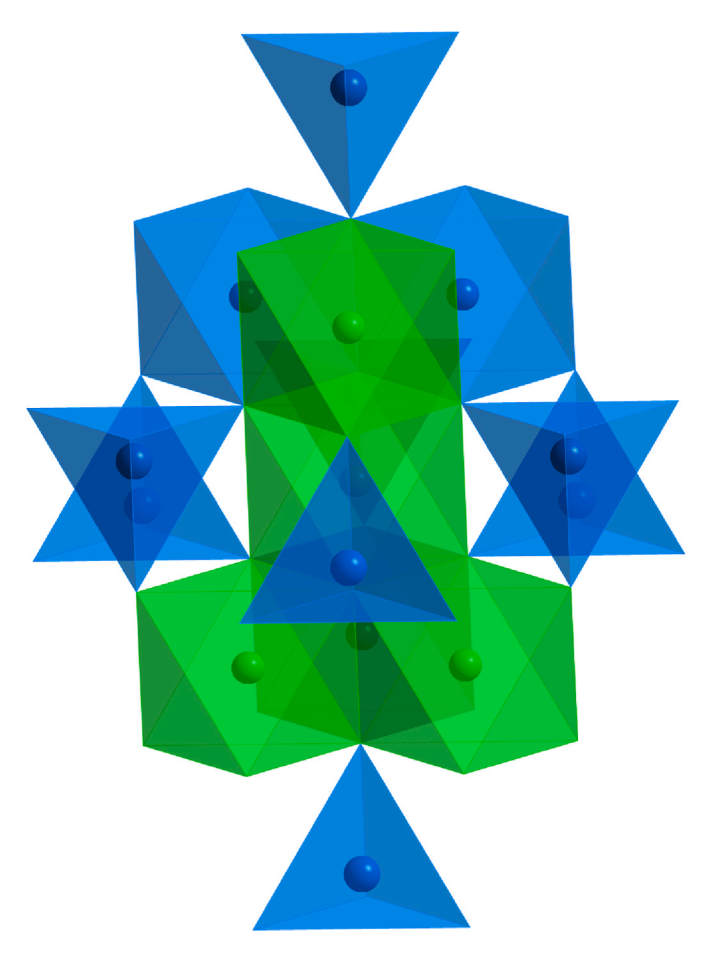


Fig. 1. Schematic of the Unit Cell of Inverse Spinel Structure $(AM_2O_4: [M]^{\text{Tetra}}[AM]^{\text{Octa}}O_4)$. AO_6 is shown by green polyhedra, MO_4 and MO_6 are shown by blue polyhedra.

 $(Mg_{2.x}Co_xSnO_4)$, while for the Zn-containing solid solutions brown $(Zn_{2.x}Co_xTiO_4)$, and green $(Zn_{2.x}Co_xSnO_4)$ shades were observed. No blue shades were obtained for the Zn-containing solid solutions despite the presence of Co^{2+} in the system, which is mainly due to the presence of the majority of chromophores at the octahedral sites.

2. Experimental

Stoichiometric amounts of MgO (CERAC, 99.5%), ZnO (Aldrich, 99.99%), TiO₂ (Aldrich, 99.9%), SnO₂ (Sigma-Aldrich, 99.9%), and CoO (Alfa, 95%) were ground in an agate mortar, pressed into pellets, and heated between 1273 and 1573 K for 12 h. Intermittent grinding and reheating were performed to ensure sample purity and homogeneity. $_x$ Co $_x$ SnO₄, and Zn_{2-x}Co $_x$ SnO₄ were x = 0.0 to 2.0. Phase purity and unit cell parameters were determined by powder XRD on a bench-top Rigaku Miniflex II powder diffractometer with Cu Kα radiation and a graphite monochromator. Time-of-flight neutron diffraction data were collected for $Mg_{2-x}Co_xTiO_4$ (x = 1.5, 2.0), $Mg_{2-x}Co_xSnO_4$ (x = 1.5, 2.0), Zn_2 . $_{x}\text{Co}_{x}\text{TiO}_{4}$ (x = 0.8, 1.5), and $\text{Zn}_{2-x}\text{Co}_{x}\text{SnO}_{4}$ (x = 0.8, 1.5) at the Oak Ridge National Laboratory (ORNL) Spallation Neutron Source (SNS) POWGEN beamline to investigate chemical composition and site distribution. Initial structures were refined using GSAS II software [18]. Magnetic measurements (2-350 K) of selected solid solutions from all four series were obtained using a Quantum Design MPMS [19]. Diffuse reflectance data (up to 2500 nm) were collected using a Jasco V-670 spectrophotometer and converted to absorbance using the Kubelka-Munk equation [20]. A Konica Minolta CM-700d spectrophotometer (standard illuminant D65) was used to measure the L*, a*, b* color coordinates [21]. Selected samples of Mg_{2-x}Co_xTiO₄, Zn_{2-x}Co_x-TiO₄, Mg_{2-x}Co_xSnO₄, and Zn_{2-x}Co_xSnO₄ were stirred in 50% HNO₃ (aq.) and 1 M NaOH for 4 h and dried, and their color properties and phase purity were determined via XRD to determine acid and base resistance.

3. Results and discussion

 Co^{2+} substitution was attempted at the M site in various M_{2-} $_{x}\text{Co}_{x}M'\text{O}_{4}$ (M = Mg/Zn, M' = Ti/Sn) inverse spinel systems. Phase pure samples were obtained for all solid solutions from (x = 0.0 to 2.0)(Fig. S1). Representative colors of the powdered samples are shown in Fig. 2. For the $Mg_{2-x}Co_xTiO_4$ (x=0.0-2.0) solid solution, the color changes from white (x = 0.0) to turquoise blue shades to green shades with increasing x. While for Mg_{2-x}Co_xSnO₄, the color evolves from white to light blue and gradually changes to dark blue and finally to green shades with increasing cobalt content. In the case of Zn-containing solid solutions, no blue hues were observed. The color of the Zn_{2-x}Co_xTiO₄ solid solution varies from white to brown to green with increasing x. The Zn_{2-x}Co_xSnO₄ solid solution shows different shades of green, evolving from light green to darker green shades with increasing x. The different shades of color observed in $Mg_{2-x}Co_xM'O_4$ and $Zn_{2-x}Co_xM'O_4$ (M' = Ti⁴⁺/Sn⁴⁺) solid solutions are apparently due to the difference in the Co–O bond distances arising from different ionic radii of Ti⁴⁺ (0.605 Å) and Sn^{4+} (0.69 Å) in octahedral coordination.

Magnetic measurements were performed on the selected M_2 $_{\chi}\text{Co}_{\chi}\text{M}'\text{O}_4$ (M=Mg/Zn,M'=Ti/Sn) inverse spinel systems to verify the oxidation state of cobalt ion. Temperature dependence of magnetic susceptibility (χ) is given in Fig. 3 (a). Using the slope and intercept of the high temperature linear region (150–350 K) of inverse magnetic susceptibility ($1/\chi$) vs. temperature plot (Fig. 3 (b), Fig. S2), Curie constants (C) and Weiss constants (θ_{W}) are determined (Table S1) All the magnetic measurements indicated the antiferromagnetic behavior in the low temperature region, with the Néel temperature (T_{N}) varying in the range of 2–44 K (Table S1). The resulting magnetic moments are higher than the expected spin-only values for a high-spin d^7 electron configuration (Table 1). However, Co^{2+} commonly has much higher measured magnetic moments due to the contribution of both spin (S) and orbital



Fig. 2. Images of selected $M_{2-x}Co_xM'O_4$ (M = Mg/Zn, M' = Ti/Sn) compounds.

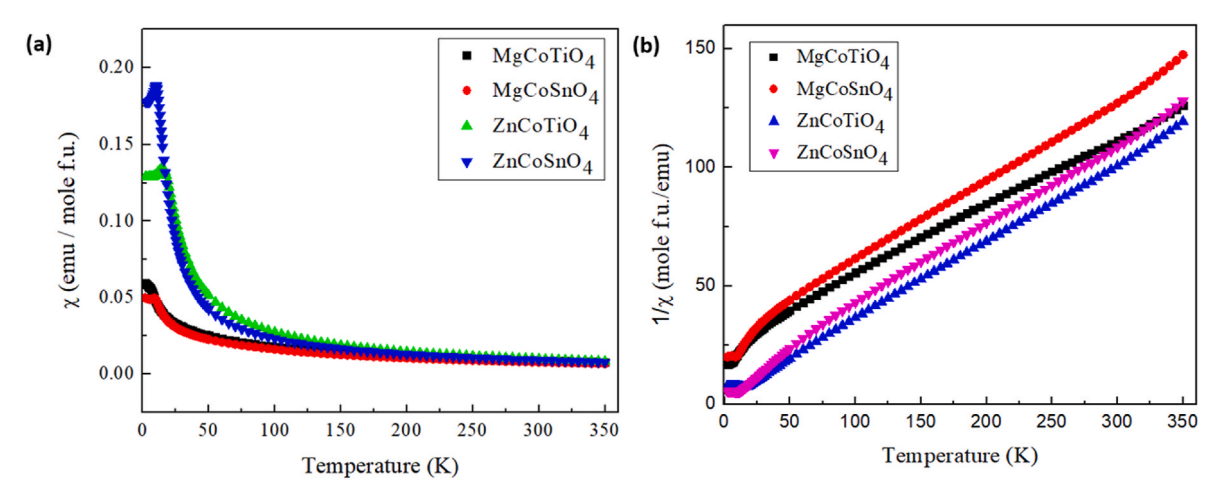


Fig. 3. (a) Magnetic susceptibility, and (b) Inverse magnetic susceptibility of $MCoM'O_4$ (M = Mg/Zn, M' = Ti/Sn) as a function of temperature. 1 emu (cgs units) = 10^{-3} A m^2 (SI units).

Table 1 Calculated spin-only, experimental, and expected magnetic moments for high spin $Co^{2+}(d^7)$ ($M_{2-x}Co_xM'O_4$ (M=Mg/Zn, M'=Ti/Sn).

Composition	$\mu_S/B.M.$ (spin only)	$\mu_{exp}/B.M.$ (Experimental)	$\mu_{S~+~L}/B.M.$ (Expected)
Mg _{1.6} Co _{0.4} TiO ₄	3.87	5.12	4.20-5.20
$Mg_{1.0}Co_{1.0}TiO_4$	3.87	5.20	4.20-5.20
$Mg_{0.5}Co_{1.5}TiO_4$	3.87	4.98	4.20-5.20
Co ₂ TiO ₄	3.87	5.09	4.20-5.20
$Zn_{1.5}Co_{0.5}TiO_4$	3.87	5.01	4.20-5.20
$Zn_{1.0}Co_{1.0}TiO_4$	3.87	5.01	4.20-5.20
$Mg_{1.9}Co_{0.1}SnO_4$	3.87	4.71	4.20-5.20
Mg _{1.5} Co _{0.5} SnO ₄	3.87	4.78	4.20-5.20
$Mg_{1.0}Co_{1.0}SnO_4$	3.87	4.84	4.20-5.20
Co ₂ SnO ₄	3.87	5.04	4.20-5.20
$Zn_{1.9}Co_{0.1}SnO_4$	3.87	4.93	4.20-5.20
$Zn_{1.5}Co_{0.5}SnO_4$	3.87	5.10	4.20-5.20
$Zn_{1.0}Co_{1.0}SnO_4$	3.87	4.93	4.20-5.20

(L), resulting in moments ranging from 4.20 to 5.20 μ_B [22,23]. Magnetic data is consistent with the interpretation that cobalt is present in the divalent state in all these phases.

Neutron structure refinements confirm that the synthesized phases are stoichiometric with no observable oxygen vacancies. In addition, bond valence sum (BVS) calculations confirm the presence of cobalt in the divalent state. The addition of Co^{2+} to the $\text{Mg}_{2,x}\text{Co}_x\text{TiO}_4$ increases

the unit cell parameters owing to the increased size of Co^{2+} over Mg^{2+} at both tetrahedral and octahedral sites, while for $\text{Zn}_{2-x}\text{Co}_x\text{TiO}_4$, the addition of Co^{2+} decreases the unit cell parameters this might be due to the different order of sizes for Co^{2+} and Zn^{2+} at both sites $(\text{Zn}^{2+}$ has a higher ionic radius than Co^{2+} at tetrahedral sites, whereas Zn^{2+} has a lower ionic radius than Co^{2+} at octahedral sites), (Fig. 4a, Table S2) [24]. $M_{2-x}\text{Co}_x\text{SnO}_4$ where M=Mg/Zn solid solutions follow the same

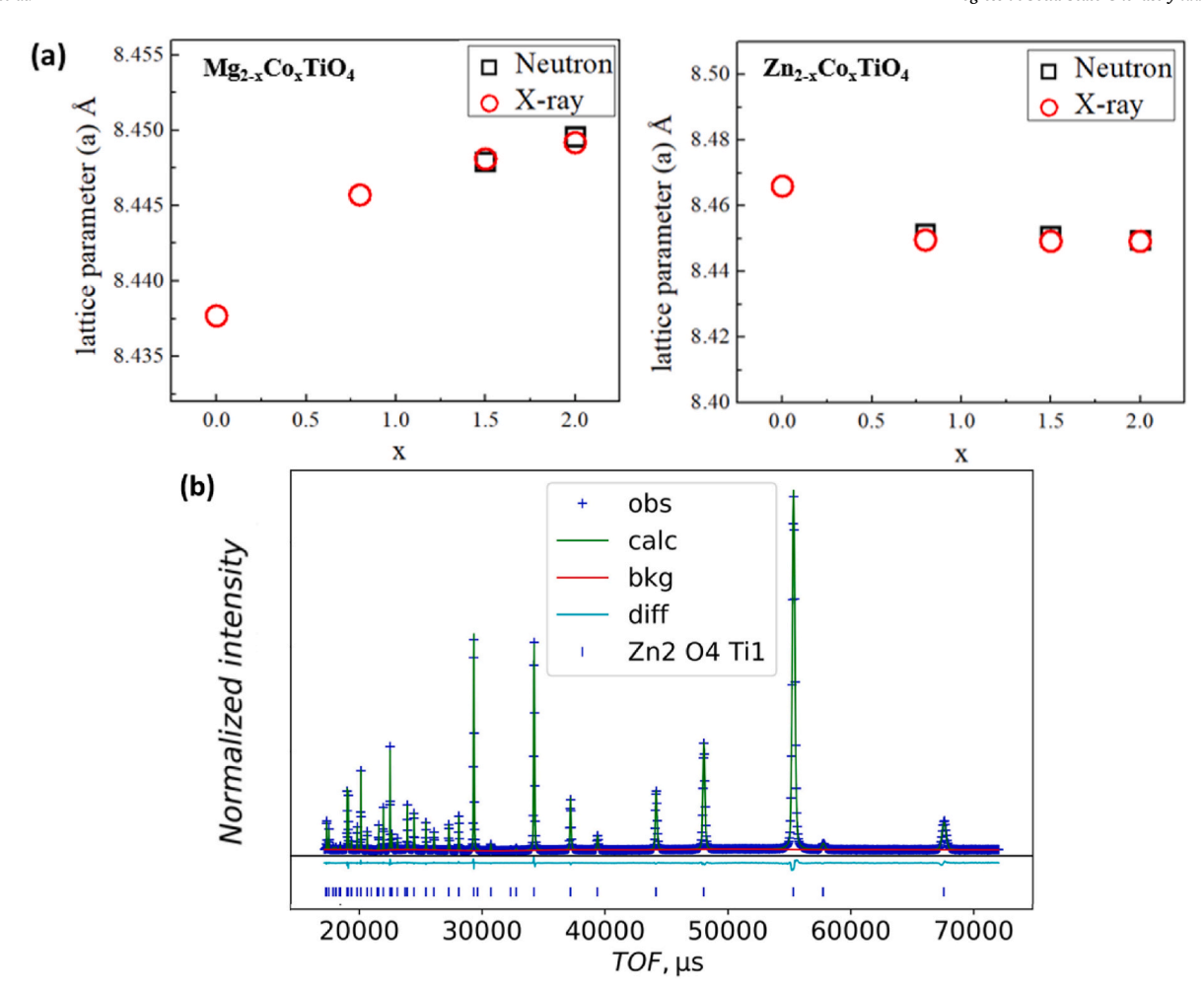


Fig. 4. (a) Lattice parameter evolution with Co²⁺ substitution in M_{2-x}Co_xTiO₄ (M = Mg/Zn) and (b) neutron Rietveld refinement of Zn_{0.5}Co_{1.5}TiO₄.

Table 2 Summary of Unit Cell and Occupancy Results by Rietveld Refinement of $M_{2-x}Co_xM'O_4$ (M=Mg/Zn, M'=Ti/Sn). The refined formula is mentioned in the SI section (S3–S9).

-							
	$\rm Mg_{0.5}Co_{1.5}TiO_4$	$\mathrm{Zn_{1.2}Co_{0.8}TiO_4}$	$Zn_{0.5}Co_{1.5}TiO_4$	$\rm Mg_{0.5}Co_{1.5}SnO_4$	$\rm Zn_{1.2}Co_{0.8}SnO_4$	$Zn_{0.5}Co_{1.5}SnO_4$	
wRp(%)	3.85	3.31	2.64	7.38	4.05	4.98	
a(Å)	8.4478(1)	8.4515(1)	8.4506(1)	8.6473(1)	8.6524(1)	8.6523(1)	
$Mg(T_d)$	0.118(5)			0.131(5)			
Mg(O _h)	0.197(1)			0.157(1)			
$Co(T_d)$	0.882(5)	0.005(7)	0.501(6)	0.869(5)	0.075(8)	0.51(1)	
Co(O _h)	0.299(1)	0.450(1)	0.459(1)	0.333(1)	0.358(6)	0.491(7)	
Ti(O _h)	0.504(1)	0.499(2)	0.520(2)				
Sn(O _h)				0.510(1)	0.5	0.5	
$Zn(T_d)$		0.995(7)	0.499(6)		0.925(8)	0.49(1)	
Zn(O _h)		0.051(1)	0.021(1)		0.142(6)	0.009(7)	

 $\label{eq:compared} \textbf{Table 3} \\ L^*a^*b^* \ color \ coordinates \ of \ Mg_{2,x}Co_xSnO_4 \ samples \ Compared \ to \ other \ well-known \ blue \ compounds.$

Composition	% mass Co	L*	a*	b*
CoAl ₂ O ₄ ^a	33.31	43.51	-4.46	-44.39
lapis lazuli stone		30.06	7.51	-24.21
$Mg_{1.8}Co_{0.2}SnO_4$	4.95	44.29	-10.32	-33.53
$Mg_{1.6}Co_{0.4}SnO_4$	9.61	36.36	-10.43	-30
$Mg_{1.4}Co_{0.6}SnO_4$	14.03	29.91	-11.17	-25.12
Mg _{1.8} Co _{0.2} SnO ₄ –HNO ₃ ^b	4.95	44.56	-10.43	-33.42
Mg _{1.8} Co _{0.2} SnO ₄ –NaOH ^b	4.95	44.39	-10.35	-33.50

^a Sample from Shepherd Color Company.

 $^{^{\}rm b}\,$ Data collected after stirring samples in 50% HNO3 (aq.) or 1 M NaOH.

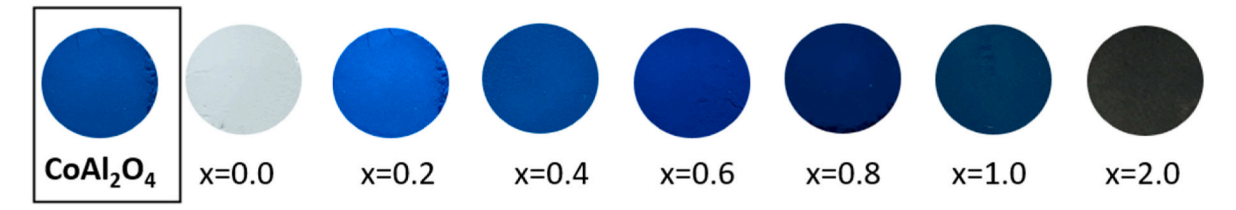


Fig. 5. Images of CoAl₂O₄ and other selected compounds of Mg_{2-x}Co_xSnO₄.

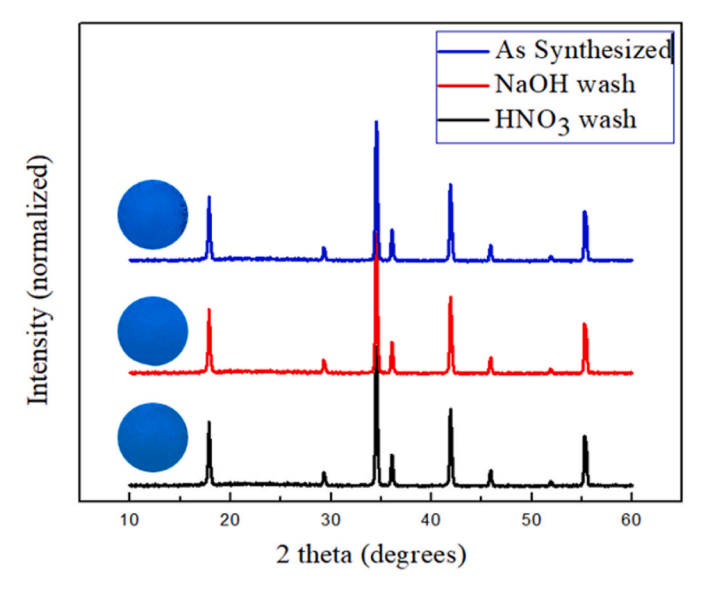


Fig. 6. XRD patterns for as-synthesized $Mg_{1.8}Co_{0.2}SnO_4$ and after acid/base tests.

order as titanium-containing series. The lattice parameters calculated from the neutron data are in good agreement with the X-ray data.

The Zn-containing solid solutions show no blue coloration for both the Ti and Sn containing series; this originates from the strong site preference of ${\rm Co^{2+}}$ substitution, affirmed by structural analysis of neutron diffraction data of ${\rm Mg_{2.x}Co_xTiO_4}$ (x=1.5) (Fig. S3), ${\rm Mg_{2.x}Co_xSnO_4}$ (x=1.5), ${\rm Zn_{2.x}Co_xTiO_4}$ (x=0.8,1.5) (Fig. 4b), and ${\rm Zn_{2.x}Co_xSnO_4}$ (x=0.8,1.5). Neutron structure analysis reveals that nearly 60% of ${\rm Co^{2+}}$ is in the tetrahedral site for ${\rm Mg_{0.5}Co_{1.5}TiO_4}$ and ${\rm Mg_{0.5}Co_{1.5}SnO_4}$, whereas 1.25, 8.85, 35, and 34% of ${\rm Co^{2+}}$ are in the tetrahedral site for ${\rm Zn_{1.2}Co_{0.8}TiO_4}$, ${\rm Zn_{1.2}Co_{0.8}SnO_4}$, ${\rm Zn_{0.5}Co_{1.5}TiO_4}$, and ${\rm Zn_{0.5}Co_{1.5}SnO_4}$ respectively (Table 2, S3-9).

The Co^{2+} ion shows a preference for tetrahedral coordination in Mgcontaining solid solutions, even though the crystal field stabilization energy for octahedral Co^{2+} is higher. This may be because the d^7 electron configuration of Co^{2+} favors a weak Jahn–Teller distortion in octahedral coordination, which is not available in these particular structures [8]. In contrast, for Zn-containing solid solutions, the strong preference of Zn for tetrahedral coordination due to sp^3 hybridization dominates over the other factor, forcing the Co^{2+} ion into octahedral coordination.

The color of these materials has been evaluated using CIE L*a*b* color space. It is a three-dimensional color model where L*a*b* uses three primary numbers to quantify the brightness (L*), green-red (a*), and blue-yellow (b*) values (Fig. S4). Higher L* values are the result of brighter colors with higher light reflectivity. Positive a* values correspond to more red coloration, while more negative b* values are more blue [21]. Mg_{2-x}Co_xSnO₄ spinel blue pigments with tunable hue give intense negative b* blue competing with that of CoAl₂O₄ (Table 3)

(Fig. 5). This tunability is rare in blue pigments and shows that these spinel pigments can be used as a versatile pigment with multiple hues to suit various needs (Fig. 5) [25,26].

To check the stability of $Mg_{2-x}Co_xSnO_4$ blue spinel samples under rigid acidic and basic conditions, a series of experiments were performed. The $Mg_{1.8}Co_{0.2}SnO_4$ composition was chosen for acid and base stability tests. Specimens of $Mg_{1.8}Co_{0.2}SnO_4$ were stirred in either 50% HNO₃ (aq.) or 1 M NaOH for 4 h, filtered, and examined via L*a*b* color measurements and X-ray diffraction (XRD). XRD patterns (Fig. 6) show no change in structure, and L*a*b* measurements reveal no change in color. This is consistent with other solid solutions in the series $Mg_{2-x}Co_xSnO_4$, which have high acid/base stability, and therefore, we believe that they are stable in most pH environments.

Neutron structure analysis reveals that Co²⁺ occupies both sites but preferentially tetrahedral sites in Mg-containing solid solutions and octahedral sites in Zn-containing solid solutions. The origin of color in all solid solutions is attributed to the d-d transition of tetrahedral and octahedral Co^{2+} . The spectroscopy of Co^{2+} in tetrahedral and octahedral coordination of oxides has been well studied. Co²⁺ in both tetrahedra and octahedra gives rise to three high-intensity peaks. One peak appears in the visible region (\sim 650 nm), and the other two appear in the NIR region (\sim 1400 nm and \sim 1600 nm). The peak around 650 nm in the visible region splits and has been explained by spin-orbit interactions of the d^7 ions [27]. Despite having the same number of peaks in both tetrahedra and octahedra, the spectra can be differentiated as Co²⁺ gives more distinct peaks in tetrahedra than in octahedra due to relaxation in the orbital selection rule. For Mg-containing solid solutions, when x is less than 1, peaks are sharp as x becomes greater than 1, peaks become more diffuse, indicating the presence of more Co²⁺ occupying octahedral sites (Fig. 7a), the opposite is observed for Zn-containing solid solution as x increases peaks become more distinct as Co^{2+} starts to occupy more of the tetrahedral sites (Fig. 7b). For Co₂TiO₄ and Co₂SnO₄, no distinct peaks are observed, although Co²⁺ is present at both sites; this might be due to broadening caused by relatively small shifting in Co²⁺ peaks for tetrahedral and octahedral sites (Fig. 7a and b).

The strong absorption in the UV region in all solid solutions results from charge transfer between metal and oxygen.

Lastly, we investigated the usefulness of $Mg_{2-x}Co_xSnO_4$ blue pigments as a near-infrared (NIR) reflective material. NIR reflectivity is a property necessary for compounds to be used as energy-saving heat reflection colorants ("cool pigments") and is the subject of increasing interest [28]. Current blue pigments containing cobalt, such as $CoAl_2O_4$, have very low NIR reflectivity. This is due to two d-d transitions for tetrahedral Co^{2+} , $^4A_2(^4F)-^4T_2(^4F)$ at 1400 nm and $^4A_2(^4F)-^4T_1(^4F)$ at 1600 nm [29]. The high concentration of Co^{2+} in $CoAl_2O_4$ gives a large absorption in the NIR region. Thus, most Co^{2+} containing compounds have very low NIR reflectivity, making them unsuitable for energy-saving coatings. The spinel blues (e.g., $Mg_{1.8}Co_{0.2}SnO_4$) show an increase in NIR reflectivity by as much as 100% between 1200 and 1600 nm and around 12.50% increase between 800 and 1000 nm while still maintaining the intense blue color (Fig. 8).

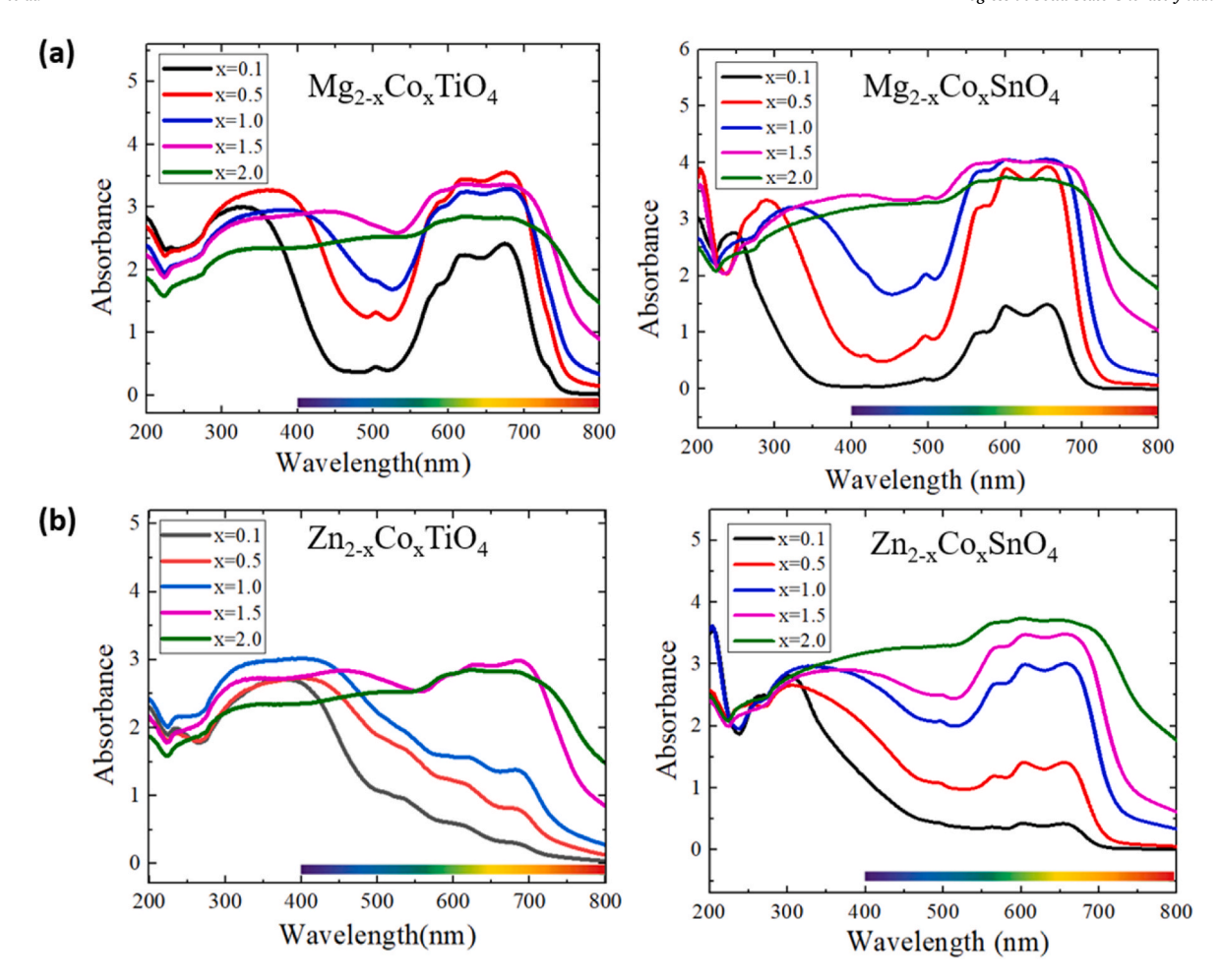


Fig. 7. (a) UV–Vis absorbance spectra of $Mg_{2x}Co_xM'O_4$ (M'=Ti/Sn) (b) UV–Vis absorbance of $Zn_{2x}Co_xM'O_4$ (M'=Ti/Sn) series.

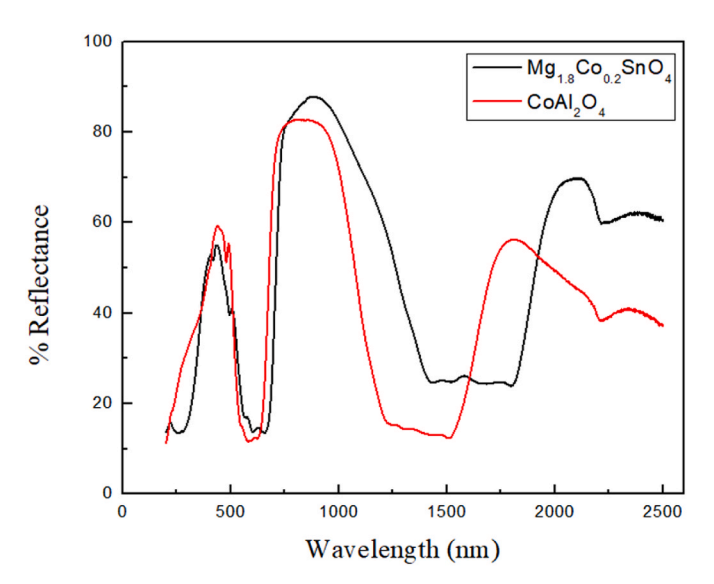


Fig. 8. NIR reflectance of $Mg_{1.8}Co_{0.2}SnO_4$. Commercial Co blue ($CoAl_2O_4$) was measured for comparison.

4. Conclusions

From prehistoric times, colored pigments have played an essential role in human civilization as they are one of the means of giving color to matter. Rationally creating an intense colorant has been a challenge for

centuries [1]. The current approaches to predicting color in new materials transcend the conventional attribution of colors to certain elements in the solid, which can often be incorrect [7].

In this study, we have shown the impact of coordination on color, where the same chromophore at different coordinations in the same structure can give rise to entirely different colors. By controlling site distribution in the system, we can design different intense pigments. Also, we have successfully created intense blue pigments with L*a*b* values similar to commercially available cobalt blue with a substantial reduction of carcinogenic cobalt from 33% to 4.9% by mass using Mg2. $_x\mathrm{Co}_x\mathrm{SnO}_4$ solid solution. It can also be used in polymer-based coatings due to its strong absorption in the UV region [30]. The pigments are stable in both acidic and basic environments, with no change in structure or color after treatment. This is comparable to the durability of both cobalt blue and YInMn blue.

Declaration of generative AI in scientific writing

The authors declare that all the responsibilities and tasks are performed by humans.

CRediT authorship contribution statement

Anjali Verma: Writing – review & editing, Writing – original draft, Investigation, Formal analysis, Conceptualization. Jun Li: Writing – review & editing, Writing – original draft, Validation, Investigation, Formal analysis. Arthur P. Ramirez: Writing – review & editing, Writing – original draft, Validation, Investigation. M.A. Subramanian: Writing – review & editing, Writing – original draft, Supervision, Project

A. Verma et al.

administration, Investigation, Funding acquisition, Formal analysis, Conceptualization.

Declaration of competing interest

The authors declare that they have no known competing financial interests or personal relationships that could have appeared to influence the work reported in this paper.

Acknowledgment

The work done at Oregon State University was supported by NSF Grant No. DMR-2025615 (M.A.S.). The work done at UC, Santa Cruz (A. P.R.) was supported by NSF Grant No. DMR-2218130. The research used resources at the Spallation Neutron Source, a DOE Office of Science User Facility operated by the Oak Ridge 12 National Laboratory (ORNL). We thank Dr. Alicia Manjon Sanz and Dr. Thomas Proffen for collecting some of the neutron diffraction data at ORNL.

Appendix A. Supplementary data

Supplementary data to this article can be found online at https://doi.org/10.1016/j.progsolidstchem.2024.100455.

References

- Subramanian MA, Li J. YInMn blue-200 Years in the making: new intense inorganic pigments based on chromophores in trigonal bipyramidal coordination. Materials Today Advances 2022;16:100323.
- [2] Burns RG. Colours of gems. Chem Brit 1983;19(12):1004-7.
- [3] Nassau K. The origins of color in minerals. Am Mineral 1978;63(3-4):219-29.
- [4] Nassau K. The fifteen causes of color. In: AZimuth, vol. 1. Elsevier; 1998.
- [5] Furukawa S, Masui T, Imanaka N. Synthesis of new environment-friendly yellow pigments. J Alloys Compd 2006;418(1–2):255–8.
- [6] Christie R. Colour chemistry. Royal society of chemistry; 2014.
- [7] Subramanian MA, Li J. Challenges in the rational design of intense inorganic pigments with desired colours. Nat Rev Mater 2023;8(2):71–3.
- [8] Duell BA, Li J, Subramanian MA. Hibonite blue: a new class of intense inorganic blue colorants. ACS Omega 2019;4(26):22114–8.
- [9] Kupferschmidt K. In search of blue. Science 2019;364:424–9.
- [10] Gehlen, A. v. F.; Thenard, V. v. B. Ueber die Bereitung einer blauen Farbe aus Kobalt, die eben so schön ist wie Ultramarin. Allg. J. Chem. 1803, 2.

- [11] Rose R, Wood N. Science and Civilisation in China, vol. 5. Cambridge University Press; 2004. p. 658–92. Part 12, Ceramic Technology (Review).
- [12] Smith AE, Mizoguchi H, Delaney K, Spaldin NA, Sleight AW, Subramanian MA. Mn³⁺ in trigonal bipyramidal coordination: a new blue chromophore. J Am Chem Soc 2009;131(47):17084–6.
- [13] Smith AE, Comstock MC, Subramanian MA. Spectral properties of the UV absorbing and near-IR reflecting blue pigment, YIn_{1-x}Mn_xO₃. Dyes Pigments 2016; 133:214–21.
- [14] Duan X, Pan M, Yu F, Yuan D. Synthesis, structure and optical properties of CoAl₂O₄ spinel nanocrystals. J Alloys Compd 2011;509(3):1079–83.
- [15] Sickafus KE, Wills JM, Grimes NW. Structure of spinel. J Am Ceram Soc 1999;82 (12):3279–92.
- [16] Ge L, Flynn J, Paddison JAM, Stone MB, Calder S, Subramanian MA, Ramirez AP, Mourigal M. Spin order and dynamics in the diamond-lattice Heisenberg antiferromagnets CuRh₂O₄ and CoRh₂O₄. Phys Rev B 2017;96(6):064413.
- [17] Wang Z, Wang Q, Wang Y, Siritanon T, Subramanian MA, Jiang P. Synthesis, properties and application of intense blue/green pigments based on Co/Cr doped Mg₂TiO₄ with excess MgO. Opt Mater 2024;148:114967.
- [18] Toby BH, Von Dreele RB. GSAS-II: the genesis of a modern open-source all purpose crystallography software package. J Appl Crystallogr 2013;46(2):544–9.
- [19] Lewis LH, Bussmann KM. A sample holder design and calibration technique for the quantum design magnetic properties measurement system superconducting quantum interference device magnetometer. Rev Sci Instrum 1996;67(10): 3537–42
- [20] El Sherif M, Bayoumi OA, Sokkar TZN. Prediction of absorbance from reflectance for an absorbing-scattering fabric. Color Res Appl 1997;22(1):32–9.
- [21] Konica Minolta I. Precise color Communication. Konica Minolta, Inc.; 2023. p. 2011–9. https://www.konicaminolta.com/instruments/knowledge/color/part 1/07.html.
- [22] Mugiraneza S, Hallas AM. Tutorial: a beginner's guide to interpreting magnetic susceptibility data with the Curie-Weiss law. Commun Phys 2022;5(1):95.
- [23] West AR. Solid state chemistry and its applications. John Wiley & Sons; 2022.
- [24] Shannon RD. Revised effective ionic radii and systematic studies of interatomic distances in halides and chalcogenides. Acta Crystallogr Sect A Cryst Phys Diffr Theor Gen Crystallogr 1976;32(5):751–67.
- [25] Li J, Lorger S, Stalick JK, Sleight AW, Subramanian MA. From serendipity to rational design: tuning the blue trigonal bipyramidal Mn³⁺ chromophore to violet and purple through application of chemical pressure. Inorg Chem 2016;55(19): 9798–804.
- [26] Li J, Subramanian MA. Inorganic pigments with transition metal chromophores at trigonal bipyramidal coordination: Y(In,Mn)O₃ blues and beyond. J Solid State Chem 2019:272:9–20.
- [27] Bates T. Ligand field theory and absorption spectra of transition-metal ions in glasses. Mod. Aspects Vitreous State 1961;2:195–254.
- [28] Jose S, Joshy D, Narendranath SB, Periyat P. Recent advances in infrared reflective inorganic pigments. Sol Energy Mater Sol Cell 2019;194:7–27.
- [29] Llusar M, Fores A, Badenes JA, Calbo J, Tena MA, Monros G. Colour analysis of some cobalt-based blue pigments. J Eur Ceram Soc 2001;21:1121–30.
- [30] Yong Q, Xu D, Liu Q, Xiao Y, Wei D. Advances in polymer-based matte coatings: a review. Polym Adv Technol 2022;33(1):5–19.